Organometallics **1991,** *10,* 1305-1310

Reaction Chemistry in the Condensation of Amine with Molybdenum-Bound Ketone and Aldehyde Complexes

Gene-Ming Yang,[†] Gene-Hsian Lee,[‡] Shie-Ming Peng,[‡] and Rai-Shung Liu*[,†]

Department of Chemistry, National Tsing Hua University, Hsinchu 30043, Taiwan, Republic of China, and Department of Chemistry, National Taiwan University, Taipei 10764, Taiwan, Republic of China

Received July 30, 1990

The reaction between $CpMo(CO)_3(\eta^1\text{-}CH_2COR)$ (R = H) (**1**), CH_3 (**2**)) and isopropylamine in the presence of $BF_3{\cdot}Et_2O$ produced the η^1-imine complexes $CpMo(CO)_3(\eta^1\text{-}CH_2CR{=}NCHMe_2)$ (R = H (**3**), CH_3 (**4**)). Decarbonylation of **3** and **4** by Me_3NO yielded the η^3-azaallyl complexes $CpMo(CO)_2(\eta^3\text{-}\mathit{CH_2CRN}CHMe_2)$ (R = H (**5**), CH_3 (**6**)). Complex **6** has been further protonated to give the corresponding iminium salt **7**. Treatment of **1** with anhydrous NH_2NH_2 in the presence of $BF_3{\cdot}Et_2O$ gave an azine complex $[CpMo(CO)_3]_2(\mu\text{-}\eta^1,\eta^1\text{-}CH_2CHNNCHCH_2\text{-})$ (**8**). Decarbonylation of the latter by Me_3NO yielded a binuclear diazaallyl complex $[CpMo(CO)_2]_2(\mu\text{-}\eta^3,\eta^3\text{-}\mathit{CH_2CHNNCHCH_2})$ (**9**). In contrast, the reaction of **2** with anhydrous NH_2NH_2 led to the formation of an acyl complex $CpMo(CO)_2(\text{-}CONHN{=}CMe_2)$ (**10**). Treatment of **1** with methylhydrazine likewise produced an analogous cyclic acyl complex $CpMo(CO)_2(\text{-}CONMeN{=}CRCH_3)$ (R = H (**11**)). Addition of $CH_3CF_3SO_3$ to **11** gives the stable carbene $[CpMo(CO)_2({=}C(OCH_3)NMeN{=}CHCH_3]CF_3SO_3$ (**12**). The molecular structures of **6**, **7**, **10**, and **12** have been determined by X-ray diffraction.

Introduction

The transition-metal η^3-allyl ligand has been shown to play an important role in many metal-mediated reactions.[1,2] Of particular interest is the complex $CpMo(NO)Cl(\eta^3\text{-allyl})$,[3] which exhibits a pattern of asymmetric metal–allyl bonding. This uncommon electronic property is responsible for its high degree of stereospecificity in the synthesis of homoallylic alcohols.[4] The key feature for this C–C bond formation is the availability of a vacant site created by the η^3–η^1 slippage.[4] In relation to this notation, it is of great interest to study the chemistry of 1-heteroallyl complexes; in these cases, the metal tends to bond asymmetrically to the ligand because of the different electronic nature of the heteroatom. Indeed, recent papers[5] have reported that molybdenum and rhenium η^3-oxaallyl complexes react facilely with alkyne and aldehyde, consequently leading to formation of the C–C bond.

In contrast with 2-azaallyl complexes,[6,7] few η^3-1-azaallyl complexes are known. Previously, Green and co-workers[8] reported that 2-substituted azirines react with $Cp_2Mo_2(CO)_4$ to yield $CpMo(CO)_2(\eta^3\text{-}\mathit{CH_2CRN}H)$. In order to provide a convenient synthesis of transition-metal–η^3-azaallyl complexes, in this paper, we report the chemistry derived from the condensation of primary amines with complexes of the type $CpMo(CO)_3(\eta^1\text{-}CH_2COR)$ (R = H (**1**), CH_3 (**2**)).[9] To our surprise, the reaction scheme is somewhat complicated and depends on the type of amines and organic carbonyls. Representative new compounds from different pathways have been characterized by X-ray diffraction analyses.

Results and Discussion

Synthesis of the η^3-Azaallyl Complexes. Addition of **1** and **2** in CH_2Cl_2 with 1 equiv of $BF_3{\cdot}Et_2O$ at −78 °C produced a red solution; further addition of isopropylamine decolored the solution, to produced the imine $CpMo(CO)_3(\eta^1\text{-}CH_2CRNCHMe_2)$ (R = H (**3**), CH_3 (**4**)). Purification of **3** and **4** was done on a silica column, from which **3** and **4** were obtained as yellow solids in a yields of 75% and 70%, respectively. For **3** and **4**, the ligand adopts an η^1-geometry, as clearly indicated by spectroscopic data. The imine carbons of **3** and **4** resonate at δ 178 and 195 ppm, respectively, and the imine hydrogen of **3** resonates at δ 7.89 ppm. The free C=N group is indicated by the

Table I. Selected Bond Distances (Å) and Angles (deg) of 6

Mo–C(6)	2.268 (6)	C(7)–N	1.353 (7)
Mo–C(7)	2.314 (5)	C(8)–C(9)	1.516 (10)
Mo–C(12)	1.930 (6)	C(8)–C(10)	1.529 (10)
Mo–C(13)	1.939 (6)	C(8)–N	1.465 (7)
Mo–N	2.215 (4)	C(12)–O(1)	1.155 (7)
C(6)–C(7)	1.413 (8)	C(13)–O(2)	1.156 (7)
C(7)–C(11)	1.501 (8)		
Mo–C(7)–N	68.6 (3)	C(6)–C(7)–C(11)	121.6 (6)
C(6)–Mo–C(13)	117.39 (22)	C(6)–C(7)–N	113.8 (5)
C(6)–Mo–N	62.23 (19)	C(11)–C(7)–N	124.5 (5)
C(7)–Mo–C(12)	89.84 (22)	C(9)–C(8)–C(10)	110.8 (6)
C(7)–Mo–C(13)	88.29 (20)	C(9)–C(8)–N	109.1 (5)
C(7)–Mo–N	34.68 (18)	C(10)–C(8)–N	108.0 (5)
C(12)–Mo–C(13)	77.34 (24)	Mo–C(12)–O(1)	178.8 (5)
C(12)–Mo–N	123.14 (21)	Mo–C(13)–O(2)	176.9 (5)
C(13)–Mo–N	87.11 (18)	Mo–N–C(7)	76.7 (3)
Mo–C(6)–C(7)	73.8 (3)	Mo–N–C(8)	127.6 (3)
Mo–C(7)–C(6)	70.3 (3)	C(7)–N–C(8)	119.9 (4)
Mo–C(7)–C(11)	126.6 (4)		

[†] National Tsing Hua University.

[‡] National Taiwan University.

[1] (a) Pearson, A. J. *Synlett* **1990**, 10. (b) Blystone, S. L. *Chem. Rev.* **1989**, *89*, 1663. (c) Faller, J. W.; Chao, K.-H. *J. Am. Chem. Soc.* **1983**, *105*, 3893. (d) Yamamoto, K.; Tsuji, J. *Tetrahedron Lett.* **1982**, *23*, 3089.

[2] (a) Trost, B. M. *Tetrahedron* **1977**, *33*, 2615. (b) Trost, B. M.; Verhoeven, T. R. *Compr. Organomet. Chem.* **1982**, *8*, 799. (c) Heck, R. F. *Palladium Reagents in Organic Synthesis*; Academic Press: New York, 1985.

[3] (a) Faller, J.-W.; John, J. A.; Mazzieri, M. R. *Tetrahedron Lett.* **1989**, *30*, 1769. (b) Faller, J. W.; Linebarrier, D. L. *J. Am. Chem. Soc.* **1989**, *111*, 1937.

[4] Adams, R. D.; Chodosh, D. F.; Faller, J. W.; Rosan, A. M. *J. Am. Chem. Soc.* **1979**, *101*, 2571.

[5] (a) Burkhardt, E. R.; Doney, J. J.; Bergman, R. G.; Heathcock, C. H. *J. Am. Chem. Soc.* **1987**, *109*, 2022. (b) Doney, J. J.; Bergman, R. G.; Heathcock, C. *J. Am. Chem. Soc.* **1985**, *107*, 3724.

[6] (a) Keable, H. R. Kilner, M. *J. Chem. Soc., Dalton Trans.* **1972**, 153. (b) Inglis, T.; Kilner, M.; Reynoldson, T.; Robertson, E. E. *Ibid.* **1975**, 924.

[7] Inglis, T.; Kilner, M. *J. Chem. Soc. Dalton Trans.* **1975**, 930.

[8] Green, M.; Mercer, R. J.; Morton, C. E.; Orpen, A. G. *Angew. Chem., Int. Ed. Engl.* **1985**, *24*, 422.

[9] (a) King, R. B.; Bisnette, M. B.; Fronzaylia, A. *J. Organomet. Chem.* **1966**, *5*, 341. (b) Ariyaratne, J. K. P.; Bierrum, A. M.; Green, M. L. H.; Ishaq, M.; Prout, C. K.; Swainwick, M. G. *J. Chem. Soc. A* **1969**, 1309.

0276-7333/91/2310-1305$02.50/0

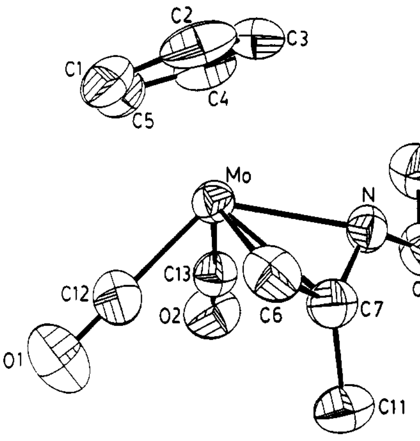

Figure 1. ORTEP drawing of **6**.

presence of the characteristic ν(C=N) absorption at ~1615 (s) cm^{-1}.

While being stirred with anhydrous Me_3NO in CH_2Cl_2, **3** and **4** readily underwent decarbonylation. Monitored by solution IR spectra, two new ν(CO) bands appeared at ~1945 (s) and 1865 (s) cm^{-1} whereas the 1615 (s) cm^{-1} band gradually disappeared. This behavior is indicative of formation of the η^3-azallyl complexes $CpMo(CO)_2(\eta^3$-*CH$_2$-CRN*CHMe$_2$) (R = H (**5**), CH_3 (**6**)). The imine hydrogen of **5** resonates at δ 4.95 ppm, ca. 2.9 ppm upfield relative to that of the η^1-complex. Notably, the magnitude of the coupling parameters J_{13} = 8.0 Hz and J_{23} = 4.8 Hz are somewhat smaller than those of common η^3-allyl complexes.[10] The imine carbons resonate at δ 116 and 132 ppm, respectively, much further upfield than those of **3** and **4**.

Single crystals of **6** were obtained by slow evaporation of a saturated ether solution at -40 °C. The ORTEP drawing is given in Figure 1, and selected bond distances and angles are provided in Table I. The molecule crystallizes in the endo conformation in which the mouth of the azaallyl group faces the Cp group.[11] In this manner, the methyl group avoids direct contact with the Cp group. The azaallyl and C(8) atoms form a perfect least-squares plane. The dihedral angle between the C(6)–C(7)–N and C(7)–N–C(8) planes is 1.3 (6)°. The C(8) atom lies 0.029 (11) Å out of the C(6)–C(7)–N plane and tilts away from the molybdenum atom. This implies that the geometry at the nitrogen approachs sp^2-hybridization, the lone pair occupying the anti position. In the azaallyl moiety, the C(6) and N atoms are clearly coordinated to the metal with bond distances of 2.268 (6) and 2.215 (4) Å, respectively. Similar to the case of $CpMo(CO)_2(\eta^3$-*CH$_2$CRN*H)[8] (R = Ph, CH_2Ph), the central carbon (Mo–C(7) = 2.314 (5) Å) is slightly further from the molybdenum than from the terminal carbon (Mo–C(6) = 2.268 (6) Å). The C(6)–C(7) (1.413 (8) Å) and C(7)–N (1.353 (7) Å) distances are intermediate between those of the corresponding single and double bonds.[12]

Molecular Structures of η^3-Iminium Complexes. The nitrogen lone pair of **6** is chemically active[8] because it can be protonated by $HBF_4{\cdot}Et_2O$ to produce an air-stable iminium compound $CpMo(CO)_2(\eta^3$-*CH$_2$-CMeCN*HCHMe$_2$)BF_4 (**7**). The two ν(Mo–CO) bands were observed at 2012 (vs) and 1936 (vs) cm^{-1}, ca. 80 cm^{-1} above those of **6**. This increase reflects an electron-attracting power that is stronger for the η^3-iminium group than for the neutral counterpart.[13] Yellow block-shaped crystals were grown from a saturated CH_2Cl_2/hexane solution. The ORTEP drawing is provided in Figure 2, and selected bond distances and angles are shown in Table II. Similar to **6**, **7** adopts an endo conformation. The two ends of the azaallyl group bond to molybdenum with the distances Mo–C(6) = 2.292 (4) Å and Mo–N = 2.215 (4) Å. In comparison with that of **6**, the Mo–C(7) bond is significantly shorter at 2.241 (4) Å and even slightly shorter than the Mo–C(6) bond (2.292 (4) Å). Moreover, the C(7)–N bond length (1.403 (4) Å) of **7** is greater than that of **6** (1.353 (7) Å) whereas the C(6)–C(7) bond (1.383 (5) Å) of **7** is shorter than that (1.413 (8) Å) of **6**. The dihedral angle between the two planes C(6)–C(7)–N and C(7)–N–C(9) is 9.9 (4) Å. The C(9) atom lies 0.215 Å out of the C(6)–C(7)–N plane and tilts away from the molybdenum atom. In this case, the positive character of molybdenum can be inferred from the two carbonyl distances. The two Mo—CO distances (1.995 (4) and 1.985 (4) Å) are slightly longer than those (1.930 (6) and 1.939 (6) Å) of **6** and the C≡O bond lengths of **1** (1.126 (5) and 1.131 (5) Å) are shorter than those (1.155 (7) and 1.156 (7) Å) of **6**. On the basis of the above comparison, if the structure of **6** represents an η^3-azaallyl

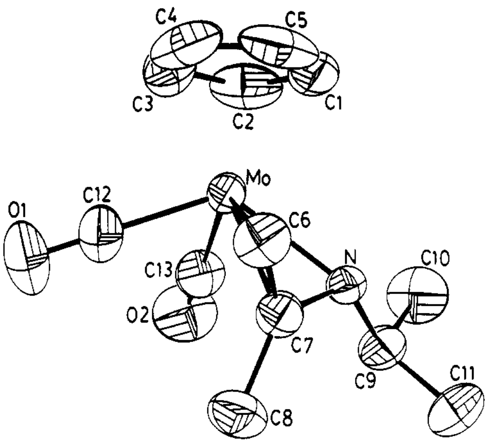

Figure 2. ORTEP drawing of **7**.

Table II. Selected Bond Distances (Å) and Angles (deg) of 7

Mo–C(6)	2.292 (4)	C(7)–N	1.403 (4)
Mo–C(7)	2.241 (3)	C(9)–C(10)	1.511 (6)
Mo–C(12)	1.995 (4)	C(9)–C(11)	1.514 (6)
Mo–C(13)	1.985 (4)	C(9)–N	1.482 (4)
Mo–N	2.231 (3)	C(12)–O(1)	1.126 (5)
C(6)–C(7)	1.383 (5)	C(13)–O(2)	1.131 (5)
C(7)–C(8)	1.496 (5)		
C(6)–Mo–C(7)	35.51 (13)	Mo–C(7)–N	71.33 (17)
C(6)–Mo–C(12)	81.46 (17)	C(6)–C(7)–C(8)	125.9 (3)
C(6)–Mo–C(13)	123.89 (16)	C(6)–C(7)–N	111.1 (3)
C(6)–Mo–N	61.03 (12)	C(8)–C(7)–N	122.8 (3)
C(7)–Mo–C(12)	85.69 (16)	C(10)–C(9)–C(11)	110.4 (4)
C(7)–Mo–C(13)	90.65 (15)	C(10)–C(9)–N	109.5 (3)
C(7)–Mo–N	36.58 (11)	C(11)–C(9)–N	109.1 (3)
C(12)–Mo–C(13)	79.52 (19)	Mo–C(12)–O(1)	180.0 (8)
C(12)–Mo–N	119.74 (15)	Mo–C(13)–O(2)	177.2 (4)
C(13)–Mo–N	84.56 (14)	Mo–N–C(7)	72.09 (17)
Mo–C(6)–C(7)	70.21 (20)	Mo–N–C(9)	129.37 (23)
Mo–C(7)–C(6)	74.27 (21)	C(7)–N–C(9)	122.1 (3)
Mo–C(7)–C(8)	126.1 (3)		

---

[10] (a) Gibson, D. H.; Hsu, W. L.; Lin, D. S. *J. Organomet. Chem.* **1979**, *172*, C7. (b) Abel, E. W.; Moorhouse, S. *J. Chem. Soc., Dalton Trans.* **1973**, 1706.

[11] (a) Davison, A.; Rode, W. C. *Inorg. Chem.* **1967**, *6*, 2125. (b) Faller, J. W.; Incorvia, M. J. *Inorg. Chem.* **1968**, *7*, 840.

[12] Huheey, J. E. *Inorganic Chemistry, Principle of Structures and Reactivity*, 3rd ed.; Harper and Row: New York, 1983.

[13] Collman, J. P.; Hegedus, L. S.; Norton, J. R.; Finke, R. G. *Principles and Applications of Organotransition Metal Chemistry*; University Science Books: Mill Valley, CA, 1987.

Scheme I

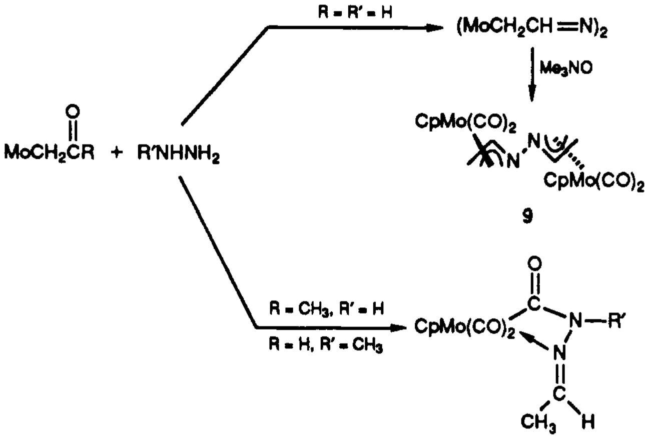

R = CH$_3$, R' = H (**10**);
R = H, R' = CH$_3$ (**11**)

bonding mode (A), metal–enamine bonding (B) is more appropriate for **7**.

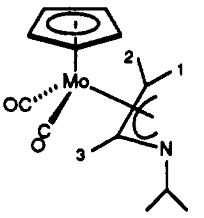

A

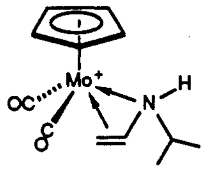

B

Reaction of 1 with Anhydrous Hydrazine. We have examined the reaction between **1** and hydrazine in the presence of BF$_3$·Et$_2$O. The reaction product was purified on a silica column to yield an orange solid, which was identified as an azine [CpMo(CO)$_3$]$_2$(μ-η^1,η^1-CH$_2$CHNNCHCH$_2$) (**8**) on the basis of elemental analysis and NMR and mass spectra. To test the possibility of hydrazone formation,[14] we have employed excess hydrazine, which nevertheless only yielded **8**. The geometry of **8** is symmetric, and the ^{1}H and ^{13}C NMR signals of the two ends of the azine ligand are equivalent. The chemical shift of the imine proton was observed at δ 8.07 ppm, and that of the imine carbon at δ 173.4 ppm. The binuclear structure was shown by a mass spectrum that displayed a two-molybdenum isotopic distribution to give the highest mass ion as 516 (^{98}Mo, M$^+$ − 2CO). Similarly, **8** readily underwent decarbonylation upon treatment with anhydrous Me$_3$NO in CH$_2$Cl$_2$ to give a red air-stable solid formulated as [CpMo(CO)$_2$(η^3-*CH$_2$CHN*)]$_2$ (**9**) (Scheme I). Complex **9** represents the first isolable μ-η^3,η^3-diazaallyl complex. The structure of **9** is supported by elemental analyses and IR, mass, and NMR data. The complex exhibits the two Mo–CO vibrations at 1940 (s) and 1885 (s) cm^{-1}. Only one diastereoisomer is detectable, probably the trans form because this minimizes the steric hindrance between the two bulky CpMo(CO)$_2$ groups. The ^{1}H and ^{13}C NMR resonances of the two ends of the ligand are equivalent and exhibit a pattern similar to **5**. The imine hydrogen resonates at δ 5.62 (dd) ppm, and the carbon resonates at δ 116 ppm. The dinuclear formula is indicated by the mass spectrum, which shows the largest mass ion of 516 (^{98}Mo, M$^+$).

Reaction of 2 with Hydrazine. An X-ray structural analysis of **9** was hampered by its poor crystallinity. Because of its novelty, we turned to synthesis of its homologue from the reaction between **2** and anhydrous hydrazine. The course of the reaction has been monitored by IR spectra. Imine formation is complete right after addition of hydrazine to the **2**–BF$_3$ mixture. The expected η^1-imine species are shown by ν(CO) bands at 2012 (s) and 1936 (s) cm^{-1} and a ν(C=N) band at ~1605 (s) cm^{-1}. It is noteworthy that during the course of stirring, a new species was formed at moderate rates and was characterized by its ν(CO) absorptions at 1946 (s), 1857 (s), and 1680 (s) cm^{-1}, but interestingly the ν(C=N) band still remained unchanged. This secondary reaction was complete in a 6-h stirring period at 23 °C. The final product was isolated in crystal form (61‰ yield) after workup. Attempts to isolate the η^1-imine intermediate encountered difficulties because of its kinetic instability in solution. The elemental analysis, mass spectrum, and IR spectrum preclude the formation of an η^3-azaallyl complex. Rather, a chelate acyl complex CpMo(CO)$_2$(CONHN=CMe$_2$) (**10**) is a more appropriate formula on the basis of the NMR spectra. The amide proton resonates at δ 10.10 ppm whereas the two methyls resonate at δ 1.94 and 2.11 ppm, respectively. The presence of an acyl group is further indicated by its ν(CO) absorption at 1680 (s) cm^{-1} and the acyl carbon resonance at 204 ppm. The imine carbon resonates at 159.2 ppm, and together with the free ν(C=N) band at 1600 cm^{-1} this information precludes the presence of a π metal–imine bonding.

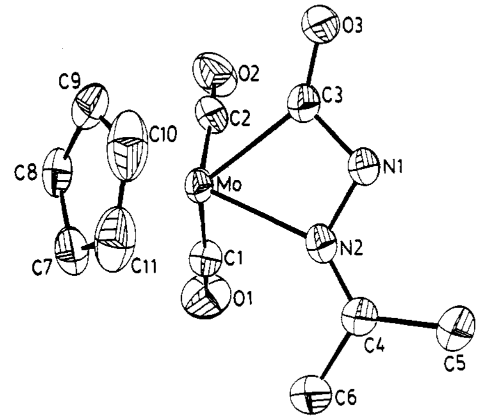

Figure 3. ORTEP drawing of **10**.

Table III. Selected Bond Distances (Å) and Angles (deg) of 10

Mo–N(2)	2.2321 (22)	N(2)–C(4)	1.275 (4)
Mo–C(1)	1.982 (4)	C(1)–O(1)	1.150 (4)
Mo–C(2)	1.940 (4)	C(2)–O(2)	1.154 (4)
Mo–C(3)	2.176 (3)	C(3)–O(3)	1.225 (4)
N(1)–N(2)	1.383 (3)	C(4)–C(5)	1.502 (4)
N(1)–C(3)	1.374 (4)	C(4)–C(6)	1.485 (4)
N(2)–Mo–C(1)	86.07 (10)	N(1)–N(2)–C(4)	121.69 (22)
N(2)–Mo–C(2)	113.72 (11)	Mo–C(1)–O(1)	176.85 (24)
N(2)–Mo–C(3)	59.91 (10)	Mo–C(2)–O(2)	176.9 (3)
C(1)–Mo–C(2)	78.08 (14)	Mo–C(3)–N(1)	98.46 (19)
C(1)–Mo–C(3)	124.10 (12)	Mo–C(3)–O(3)	140.23 (21)
C(2)–Mo–C(3)	77.69 (12)	N(1)–C(3)–O(3)	121.24 (25)
N(2)–N(1)–C(3)	105.97 (21)	N(2)–C(4)–C(5)	123.5 (3)
Mo–N(2)–N(1)	95.65 (15)	N(2)–C(4)–C(6)	119.0 (3)
Mo–N(2)–C(4)	142.63 (20)	C(5)–C(4)–C(6)	117.5 (3)

The molecular structure of **10** is further elucidated by means of X-ray diffraction. An ORTEP drawing is provided in Figure 3, and selected bond distances and angles are given in Table III. The molybdenum atom forms a four-member ring with C(3) and N(2) as the chelating atoms. The least-squares plane defined by the four-member ring is planar with a maximum deviation of 0.002 Å,

---

[14] Casey, F. A.; Sundberg, R. J. *Advanced Organic Chemistry*; Plenum Press: New York, 1979.

and the C(4) and O(3) atoms lie −0.034 (6) and −0.052 (6) Å out of the plane, respectively (the negative values refer to atoms tilted away from the Cp group). The Mo—C(3) bond distance of 2.176 (3) Å is significantly smaller than the accepted values (2.28–2.33) of a normal Mo—C single bond,[15] but larger than that (1.90–1.95) of a normal double bond.[16] The C(3)—O(3) distance (1.225 (4) Å) is slightly greater than that of a standard CO double bond (1.20 Å). In contrast, the C(3)—N(1) (1.374 (4) Å) and N(1)—N(2) (1.383 (3) Å) bond lengths are smaller than those of the common single C—N (1.47 Å) and N—N (1.45 Å) bond lengths, whereas the C(4)—N(2) length (1.275 (4) Å) is comparable to that observable for a normal CN double bond (1.25 Å). The Mo—N(2) distance (2.232 (2) Å) is reasonable in comparison with those (2.20–2.25 Å) observed for $(\eta^3\text{-}C_5H_7)Mo(CO)_2(CH_3CN)_2Br$,[17] $[(\eta^3\text{-}C_3H_5)Mo(CH_3CN)_2(CO)_2]^+$,[18] and $MoCl(CO)_2(CyN{=}CHCH{=}NCy)(\eta^3\text{-}C_4H_7)$.[19] The data above are indicative of the resonance pattern within the four-member ring shown in Scheme II. Further participation of imine π electrons for further resonances is considered unlikely, as no significant decrease in the N(2)–C(4) bond length is observable. The coplanarity of the imine carbon and the four-member ring is simply due to the sp²-hybridization nature of the imine group.

An analogous acyl complex **11** was also obtained from the reaction of **1** and methylhydrazine. The complex was present as yellow crystals after workup (52% yield). The ^1H and ^{13}C NMR spectra exhibited a pattern similar to those of **10** notably; the methyl is found trans to the NMe fragment, as shown by an X-ray study of its carbenium derivative (vide post).

A hydrazone is believed to be the intermediate for formation of the chelate acyl complexes. In fact, for **10**, the hydrazone intermediate has been detected by solution IR spectra; further characterization of this species by NMR spectra was not successful because of the impurity of crude product. Nevertheless, its existence was confirmed by mass spectra, which showed the highest mass ion of (^{98}Mo, 290). In the case of **10**, no azine forms, since further condensation of hydrazone with ketone is less likely than for aldehyde. The stereochemistry of **11** helps to clarify the mechanism. We propose that the Mo–C bond is first cleaved by the NH group intermolecularly to give a zwitterion. The NR^- end of the latter subsequently undergoes intramolecular CO insertion to give the four-member ring.

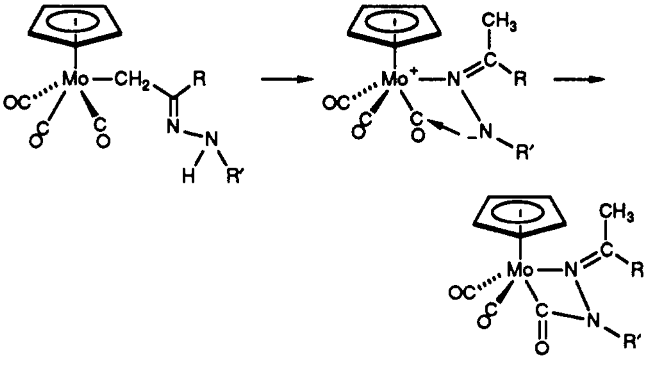

Scheme II

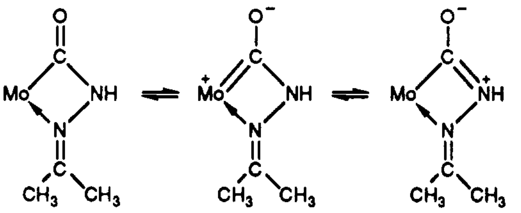

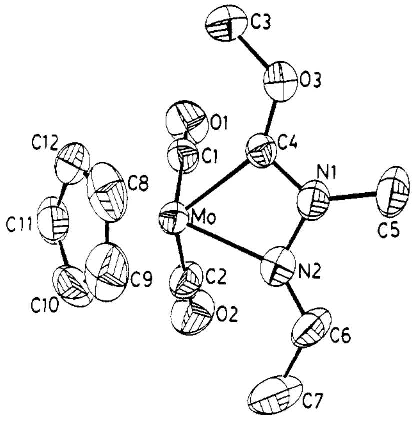

Figure 4. ORTEP drawing of 12.

Table IV. Selected Bond Distances (Å) and Angles (deg) of 12

Mo–N(2)	2.207 (3)	N(2)–C(6)	1.272 (4)
Mo–C(1)	1.953 (3)	O(1)–C(1)	1.147 (4)
Mo–C(2)	1.991 (4)	O(2)–C(2)	1.149 (4)
Mo–C(4)	2.141 (3)	O(3)–C(3)	1.456 (4)
N(1)–N(2)	1.386 (4)	O(3)–C(4)	1.304 (4)
N(1)–C(4)	1.331 (4)	C(6)–C(7)	1.457 (5)
N(1)–C(5)	1.457 (4)		
N(2)–Mo–C(1)	113.30 (11)	Mo–N(2)–C(6)	143.09 (23)
N(2)–Mo–C(2)	82.65 (11)	N(1)–N(2)–C(6)	120.5 (3)
N(2)–Mo–C(4)	58.79 (11)	C(3)–O(3)–C(4)	118.98 (23)
C(1)–Mo–C(2)	77.22 (13)	Mo–C(1)–O(1)	178.7 (3)
C(1)–Mo–C(4)	80.48 (11)	Mo–C(2)–O(2)	179.2 (3)
C(2)–Mo–C(4)	121.89 (12)	Mo–C(4)–N(1)	101.27 (20)
N(2)–N(1)–C(4)	103.55 (23)	Mo–C(4)–O(3)	144.02 (21)
N(2)–N(1)–C(5)	125.34 (25)	N(1)–C(4)–O(3)	114.7 (3)
C(4)–N(1)–C(5)	131.1 (3)	N(2)–C(6)–C(7)	121.1 (3)
Mo–N(2)–N(1)	96.35 (17)		

Because of the transoid nature of η^1-hydrazone, direct cyclization by intramolecular NMR′ addition to the carbonyl is unlikely to occur. We cannot preclude the possibility of an intermolecular process involving the hydrazone addition to the carbonyl of a second metal complex.

Preparation of the Carbenium Complexes. The availability of the acyl complex allows the synthesis of a Fischer-type carbenium. Treatment of **11** with $CH_3CF_3SO_3$ in CH_2Cl_2 produced the air-stable cation $[CpMo(CO)_2({=}CC(OCH_3)NMeN{=}CHMe)]CF_3SO_3$ (**12**) in good yield. The anion was replaced with the BPh_4^- anion, and block-shaped red crystals were grown from a saturated CH_2Cl_2/hexane solution. Its infrared spectrum exhibits two ν(Mo—CO) bands at 1988 (s) and 1900 (s) cm⁻¹, about 40–50 cm⁻¹ above those of **11**. The Mo=C carbon resonates at δ 324.3 ppm, typical of a carbenium carbon.[20]. The solid-state structure has been characterized by means of an X-ray diffraction study. An ORTEP diagram is provided in Figure 4, and selected bond distances and angles

---

[15] Bennett, M. J.; Mason, R. *Proc. Chem. Soc.* **1963**, 273.

[16] Green, M.; Norman, N. C.; Orpen, A. G. *J. Am. Chem. Soc.* **1981**, *103*, 1269.

[17] Lee, G. H.; Peng, S. M.; Liu, F. C.; Mu, D.; Liu, R. S. *Organometallics* **1989**, *8*, 402.

[18] Drew, M. G. B.; Brisdon, B. J.; Cartwright, M. *Inorg. Chim. Acta* **1979**, *36*, 127.

[19] Graham, A. J.; Akrigg, D.; Sheldrick, B. *Cryst. Struct. Commun.* **1976**, *5*, 891.

[20] Buhro, M. E.; Wong, A.; Merrifield, J. H.; Liu, G. Y.; Constable, A. G.; Gladysz, J. A. *Organometallics* **1988**, *2*, 1852.

Scheme III

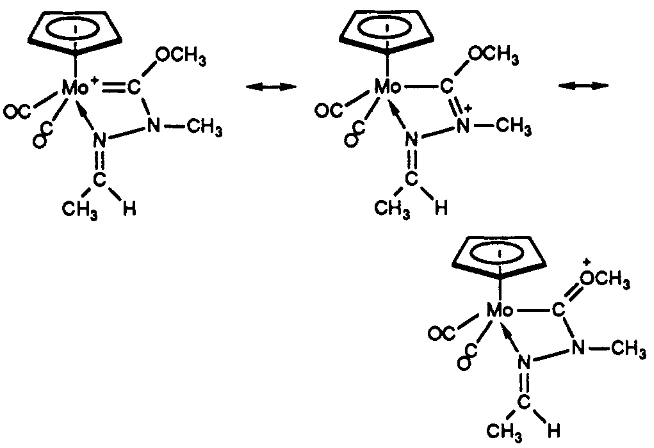

are given in Table IV. Similar to **10**, the molybdenum atom bonds the C(4) and N(2) atoms to form a four-member ring. The C(7) atom lies trans to the N(1) atom with respect to the N(2)—C(6) double bond. The Mo—C(4) bond length (2.14 (3) Å) is comparable to that (2.176 (3) Å) of **10** and represents an intermediate value between Mo—C single (2.30 Å) and double (1.95 Å) bonds. Relative to **10**, the C(4)—O(3) bond length is increased to 1.304 (4) Å whereas the C(4)—N(1) bond is slightly decreased to 1.331 (4) Å. The Mo—N(2) bond length (2.207 (3) Å) is slightly shorter than that (2.232 (2) Å) of **10**. The set of atoms including the ring, C(6), and O(3) carbons is planar with a maximum deviation of 0.06 Å. All the data here imply that the cation **12** can be represented by the standard Fischer carbenium resonances given in Scheme III.

Experimental Section

All operations were carried out under argon in a Schlenk apparatus or in a glovebox. Diethyl ether, tetrahydrofuran, and pentane were dried with sodium/benzophenone and distilled before use. Dichloromethane, chloroform, and acetonitrile were dried over phosphorus pentoxide and distilled. Anhydrous hydrazine, methyl hydrazine, trimethylamine oxide, and molybdenum hexacarbonyl were obtained from Strem and used without purification. Complexes **1** and **2**[9], and CpMo(CO)$_3$Na[9] were prepared according to the literature methods.

All ^{1}H (400 MHz) and ^{13}C (100 MHz) NMR spectra were recorded on a Bruker AM-400 spectrometer. The ^{1}H and ^{13}C NMR spectra were referenced to tetramethylsilane. Infrared spectra were recorded on a Perkin-Elmer 781 spectrophotometer. Microanalyses were performed at the Microanalytic Laboratory at National Taiwan University.

Synthesis of CpMo(CO)$_3$(η^1-CH$_2$CH=NCHMe$_2$) (3). Complex **1** (0.52 g, 2.00 mmol) was dissolved in 20 mL of THF to which was added BF$_3$·Et$_2$O (0.28 g, 2.01 mmol) at −78 °C. To this red stirred solution was added isopropylamine (0.11 g, 2.00 mmol), and the solution turned yellow. The mixture was stirred at −78 °C for 6 h. After removal of the solvent to dryness, the residue was chromatographed through a silica column by using ether/hexane (1:1 volume ratio) as the eluting solvent. After elution of the first purple band of [CpMo(CO)$_3$]$_2$, a yellow band was collected and evaporated to dryness to give a yellow solid of **1** (75% yield, 0.50 g, 1.50 mmol). IR (CH$_2$Cl$_2$), cm^{-1}: ν(CO) 2048 (vs), 1950 (vs); ν(C=N) 1615 (s). Mass (12 eV, ^{98}Mo), *m/z*: 331 (M$^+$). ^{1}H NMR (400 MHz, CDCL$_3$), δ: 1.28 (d, 6 H, 2 CH$_3$), 2.37 (d, 2 H, CH$_2$), 3.82 (m, 1 H, CHMe$_2$), 5.56 (s, 5 H, C$_5$H$_5$), 7.89 (t, 1 H, C*H*N), $J_{\mathrm{CH_2\text{-}CHN}}$ = 8.6 Hz, $J_{\mathrm{H\text{-}CH_3}}$ = 6.6 Hz. ^{13}C NMR (100 MHz, CDCl$_3$), δ: 1.61 (CH$_2$), 21.79 (CH$_3$), 53.8 (*C*HMe$_2$), 94.0 (C$_5$H$_5$), 178 (*C*=N), 227.0, 236 (2 Mo—CO). Anal. Calcd for C$_{13}$H$_{15}$MoO$_3$N: C, 47.43; H, 4.59; N, 4.25. Found: C, 47.23; H, 4.48; N, 4.29.

Synthesis of CpMo(CO)$_3$(η^1-CH$_2$CMe=NCHMe$_2$) (4). This complex was similarly prepared from the reaction of **2** with isopropylamine in the presence of BF$_3$·Et$_2$O; the yield is 70%. IR (CH$_2$Cl$_2$), cm^{-1}: ν(CO) 2044 (vs), 1952 (vs); ν(C=N) 1620 (s). Mass (12 eV, ^{98}Mo), 345 *m/z*: (M$^+$). ^{1}H NMR (400 MHz, CDCL$_3$): 1.28 (6 H, d, 2 CH$_3$), 2.08 (s, 3 H, CH$_3$), 2.09 (s, 2 H, CH$_2$), 3.40 (m, 1 H, C*H*Me$_2$), 5.35 (5 H, s, C$_5$H$_5$), $J_{\mathrm{H\text{-}CH_3}}$ = 6.6 Hz. ^{13}C (100 MHz), δ: 3.91 (CH$_2$), 21.5 (CH$_3$), 22.5 (CH$_3$), 49.4 (*C*HMe$_2$), 94.5 (C$_5$H$_5$), 197.0 (C=N), 228.7 and 229.7 (2 Mo—CO). Anal. Calcd for C$_{14}$H$_{17}$MoO$_3$N: C, 48.99; H, 4.99; N, 4.08. Found: C, 48.91; H, 4.89; N, 4.12.

Synthesis of CpMo(CO)$_2$(η^3-*CH$_2$CHN*CHMe$_2$) (5). Complex **3** (0.50 g, 1.50 mmol) was stirred with Me$_3$NO (0.11 g, 1.5 mmol) in 20 mL of CH$_2$Cl$_2$ for 6 h. Afer removal of the solvent, the residue was chromatographed through a silica column with ether/hexane (1:1) as the eluting solvent. A brown band was developed, collected, and evaporated to dryness to yield a dark brown solid. Further recrystallization from a saturated CH$_2$Cl$_2$/hexane solution yielded block-shaped brown crystals (67% yield, 0.30 g, 1.00 mmol). IR (CH$_2$Cl$_2$), cm^{-1} ν(CO) 1945 (vs) 1865 (s) cm^{-1}. Mass (12 eV, ^{98}Mo), *m/z*: 303 (M$^+$). ^{1}H NMR (400 MHz, CDCl$_3$), δ: 1.25 (d, 3 H, CH$_3$), 1.28 (d, 3 H, CH$_3$), 2.39 (d, 1 H, H^1), 2.75 (d, 1 H, H^2), 4.95 (dd, 1 H, H^3), 5.43 (s, 5 H, C$_5$H$_5$), J_{13} = 8.0 Hz, J_{23} = 1.8 Hz, $J_{\mathrm{CH_3\text{-}H}}$ = 4.9 Hz. ^{13}C NMR (100 MHz, CDCl$_3$), δ: 25.9 (CH$_3$), 28.8 (CH$_3$), 30.5 (CH^{1}H^2), 61.7 (*C*HMe$_2$), 116.2 (CH^3), 247.4, 245.8 (2 Mo–CO). Anal. Calcd for C$_{12}$H$_{15}$MoO$_2$N: C, 48.01; H, 4.70; N, 4.67. Found: C, 47.92; H, 4.62; N, 4.83.

Synthesis of CpMo(CO)$_2$(η^3-*CH$_2$CMeN*CHMe$_2$) (6). This complex was prepared similarly from decarbonylation of **4** with Me$_3$NO; the yield is 52%. IR (CH$_2$Cl$_2$), cm^{-1}: ν(CO) 1937 (vs), 1845 (vs). Mass (12 eV, ^{98}Mo), *m/z*: 317 (M$^+$). ^{1}H NMR (400 MHz, CDCl$_3$), δ: 1.17 (d, 3 H, CH$_3$), 1.35 (d, 3 H, CH$_3$), 1.85 (s, 3 H, CH$_3$), 2.16 (s, 1 H, H^1), 2.78 (s, 1 H, H^2), 3.14 (m, 1 H, CHMe$_2$), 5.45 (s, C$_5$H$_5$), J_{CHMe} = 6.0 Hz. ^{13}C NMR (100 MHz, CDCl$_3$), δ: 15.92 (CH$_3$), 24.7 (CH$_3$), 26.7 (CH$_3$), 31.8 (CH^{1}H^2), 53.6 (*C*HMe$_2$), 94.8 (C$_5$H$_5$), 132.4 (*C*=N), 246.5 and 247.4 (2 Mo—CO). Anal. Calcd for C$_{13}$H$_{17}$MoO$_2$: C, 49.53; H, 5.44; N, 4.44. Found: C, 49.25; H, 5.62; N, 4.64.

Synthesis of CpMo(CO)$_2$(η^3-*CH$_2$CMeNH*CHMe$_2$)BF$_4$ (7). Complex **6** (0.50 g, 1.50 mmol) was dissolved in 15 mL of ether, and 0.25 g of HBF$_4$·Et$_2$O (1.60 mmol) was added to yield an orange precipitate. After collection by filtration, the precipitate was washed with 20 mL of ether and further recrystallized from CH$_2$Cl$_2$/ether to produce orange block crystals. IR (CH$_2$Cl$_2$), cm^{-1}: ν(CO) 2012 (s), 1936 (s). ^{1}H NMR (400 MHz, CDCl$_3$), δ: 1.25 (d, 3 H, CH$_3$), 1.45 (d, 3 H, CH$_3$), 1.83 (br s, 1 H, NH), 2.54 (s, 3 H, CH$_3$), 3.03, 3.04 (s, s, 2 H, ^{1}H + ^{2}H), 3.15 (m, 1 H, CHMe$_2$), 5.76 (s 5 H, C$_5$H$_5$). ^{13}C NMR (100 MHz, CDCl$_3$), δ: 18.9, 22.8, 23.3 (3 CH$_3$), 40.4 (CH^{1}H^2), 54.1 (*C*HMe$_2$), 94.6 (C$_5$H$_5$), 232.3 (2 CO). Anal. Calcd for C$_{14}$H$_{18}$MoO$_3$NBF$_4$: C, 41.72; H, 4.50; N, 3.47. Found: C, 41.86; H, 4.42; N, 3.50.

Synthesis of [CpMo(CO)$_3$]$_2$(μ-η^1,η^1-CH$_2$CHNNCHCH$_2$) (8). To complex **1** (0.50 g, 1.70 mmol) in 20 mL of CH$_2$Cl$_2$ was added BF$_3$·Et$_2$O (0.24 g, 1.70 mmol) at −78 °C to give a red solution. Anhydrous hydrazine (0.11 g, 3.4 mmol) was added, and the mixture was stirred for 6 h. After removal of the solvent under reduced pressure, the residues were chromatographed through a silica column by using ether/hexane (1:1 volume ratio) as the eluting solvent. After elution of the unwanted purple band of [CpMo(CO)$_3$]$_2$, a brown band developed and was collected, producing a dark orange solid of **8** (59%, 0.57 g, 1.00 mmol). IR (CH$_2$Cl$_2$), cm^{-1}: ν(CO) 2050 (vs), 1950 (vs); ν(C=N) 1600 (s). Mass (12 eV, ^{98}Mo), *m/z*: 516 (M$^+$ − 2CO). ^{1}H NMR (400 MHz, CDCl$_3$), δ: 2.24 (d, 2 H, CH$_2$), 5.34 (s, 5 H, C$_5$H$_5$), 8.07 (t, 1 H, CH=N). ^{13}C NMR (100 MHz, CDCl$_3$), δ: 29.7 (CH$_2$), 92.1 (C$_5$H$_5$), 171.4 (C=N), 216.4, 226.9 (2 Mo—CO). Anal. Calcd for C$_{20}$H$_{16}$Mo$_2$O$_6$N$_2$: C, 41.98; H, 2.82; N, 4.89. Found: C, 42.05; H, 2.86; N, 4.95.

Synthesis of [CpMo(CO)$_2$]$_2$(μ-η^3,η^3-*CH$_2$CHNNCHCH$_2$*) (9). Complex **8** (1.0 g, 1.70 mmol) in 20 mL of CH$_2$Cl$_2$ was stirred with Me$_3$NO (0.26 g, 3.40 mmol) for 6 h. After removal of the solvent, the residue was chromatographed through a silica column by using ether/hexane as the eluting solvent. After elution of the unwanted purple band of [CpMo(CO)$_3$]$_2$, the dark red immobile band remaining at the top of the column was eluted with THF to give a dark orange band, which was collected and evaporated to dryness to give a dark red crystalline solid (50% yield, 0.52 g, 1.00 mmol). IR (CH$_2$Cl$_2$), cm^{-1}: ν(CO) 1940 (vs), 1885 (vs). Mass (12 eV, ^{98}Mo),

Table V. Summary of Crystal Data and Data Collection

compd	**6**	**7**	**10**	**12**
empirical formula	$C_{13}H_{17}O_2NMo$	$C_{13}H_{18}O_2NBF_4Mo$	$C_{11}H_{12}O_3N_2Mo$	$C_{36}H_{35}O_3N_2BMo$
cryst size, mm	0.30 × 0.30 × 0.50	0.40 × 0.60 × 0.60	0.12 × 0.40 × 0.50	0.40 × 0.50 × 0.60
space group	orthorhombic; *Pbac*	monoclinic; $P2_1/c$	monoclinic; $P2_1/c$	monoclinic; $P2_1/c$
cell dimens				
a, Å	15.153 (5)	7.092 (1)	7.162 (2)	10.844 (7)
b, Å	13.535 (5)	14.824 (4)	25.471 (5)	13.642 (2)
c, Å	13.354 (4)	15.964 (4)	7.566 (5)	21.805 (4)
β, deg		102.20 (2)	116.70 (4)	95.28 (4)
υ, $Å^3$	2739 (2)	1640.9 (6)	1233.1 (9)	3212 (2)
Z	8	4	4	4
fw	315.22	403.03	310.12	650.43
d(calc), Mg/m^3	1.529	1.631	1.670	1.345
abs coeff, mm^{-1}	0.92	0.82	1.04	0.43
F(000)	1279.51	807.74	631.74	1343.65
diffractometer	Enraf-Nonius, CAD4	Enraf-Nonius, CAD4	Enraf-Nonius, CAD4	Enraf-Nonius, CAD4
λ(Mo K*α* radiation), Å	0.7093	0.7093	0.7093	0.7093
T, K	room temp	room temp	room temp	room temp
monochromator	highly oriented graphite crystal	highly oriented graphite crystal	highly oriented graphite crystal	highly oriented graphite crystal
2*θ* range, deg	2.0–50.0	2.0–50.0	2.0–50.0	2.0–50.0
scan type	$\theta/2\theta$	$\theta/2\theta$	$\theta/2\theta$	$\theta/2\theta$
scan speed (*θ*), deg/min	1.20–8.24	0.98–8.24	0.98–8.24	1.05–8.24
scan range (*θ*), deg	$0.80 + 0.35 \tan \theta$	$0.65 + 0.35 \tan \theta$	$0.65 + 0.35 \tan \theta$	$0.70 + 0.35 \tan \theta$
std reflns	3 measured/2 h	3 measured/2 h	3 measured/2 h	3 measured/2 h
(variation)	(<2%)	(<4%)	(<2%)	(<2%)
index ranges	$0 \le h \le 18, 0 \le k \le 16, 0 \le l \le 15$	$-9 \le h \le 8, 0 \le k \le 19, 0 \le l \le 20$	$-8 \le h \le 7, 0 \le k \le 30, 0 \le l \le 8$	$12 \le h \le -12, 0 \le k \le 16, 0 \le l \le 25$
no of reflns collcd	2396	4065	2334	5896
ind reflns	2396 ($1591 > 2.0\sigma(I)$)	3758 ($2961 > 2\sigma(I)$)	2162 ($1853 > 2\sigma(I)$)	5590 ($4551 > 2\sigma(I)$)
T_{min}/T_{max}	0.817/0.993	0.852/0.999	0.814/0.999	0.969/1.000
soln	Patterson methods	Patterson Methods	Patterson Methods	Patterson Methods
hydrogen atom	fixed refinement flag	same	same	same
weighting scheme	$w^{-1} = \sigma^2(F)$	$w^{-1} = \sigma^2(F) + 0.0001F^2$	$w^{-1} = \sigma^2(F)$	$w^{-1} = \sigma^2(F)$
final *R* indices, %	$R = 3.1, R_w = 2.5$	$R = 3.3, R_w = 4.5$	$R = 2.2, R_w = 2.1$	$R = 3.1, R_w = 2.7$
goodness-of-fit	1.89	2.34	2.26	2.76
largest and mean c/s	0.44, 0.001	0.279, 0.001	0.025, 0.001	0.315, 0.001
data/params	7.17/1	14.8/1	12.0/1	11.7/1
largest peak, c/$Å^3$	0.35	0.55	0.27	0.28
largest hole, c/$Å^3$	−0.45	−0.49	−0.32	−0.37

m/z: 516 (M^+). ^1H NMR (400 MHz, $CDCl_3$), *δ*: 2.18 (d, 1 H, H^1), 2.54 (d, 1 H, H^2), 5.42 (s, 5 H, C_5H_5), 5.62 (dd, 1 H, H^3). ^{13}C NMR (100 MHz, $CDCl_3$), *δ*: 25.8 (CH^1H^2), 94.4 (C_5H_5), 116.1 (CH^3), 224.0, 248.0 (2 Mo—CO). Anal. Calcd for $C_{18}H_{16}Mo_2O_4N_2$: C, 41.87; H, 3.12; N, 5.43. Found: C, 41.80; H, 3.09; N, 5.45.

Synthesis of $CpMo(CO)_2(\text{-CONHN=CMe}_2)$ (10). To complex 2 (0.50 g, 1.70 mmol) in 20 mL of CH_2Cl_2 was added $BF_3{\cdot}Et_2O$ (0.24 g, 1.70 mmol) at −78 °C to produce a dark red solution. Anhydrous hydrazine (0.11 g, 3.40 mmol) was added, and the mixture was stirred for 6 h. After removal of the solvent under reduced pressure, the residues were chromatographed through a silica column by using ether/hexane (1:1 volume ratio) as the eluting solvent. After elution of the unwanted purple band of $[CpMo(CO)_3]_2$, the yellow immobile band at the top of the column was eluted with CH_2Cl_2, collected, and evaporated to dryness to give a yellow orange solid. Crystallization from CH_2Cl_2/hexane produced dark orange crystals (64% yield, 0.34 g, 1.10 mmol). IR (CH_2Cl_2), cm^{-1}: *ν*(CO) 1946 (vs), 1857 (vs), 1680 (vs); *ν*(C=N) 1600 (vs). Mass (12 eV, ^{98}Mo), *m/z*: 318 (M^+). ^1H NMR (400 MHz, $CDCl_3$), *δ*: 1.94 (s, 3 H, CH_3), 2.11 (s, 3 H, CH_3), 5.46 (s, 5 H, C_5H_5), 10.10 (s, 1 H, NH). ^{13}C NMR (100 MHz, $CDCl_3$), *δ*: 17.0 (CH_3), 25.9 (CH_3), 93.8 (C_5H_5), 160.0 (C=N), 204.6 (*C*O—NH), 245.0, 254 (2 Mo—CO). Anal. Calcd for $C_{11}H_{12}MoO_3N_2$: C, 41.78; H, 3.82; N, 8.86. Found: C, 41.80; H, 3.86; N, 8.89.

Synthesis of $CpMo(CO)_2(\text{-CONMeN=CHCH}_3)$ (11). This complex was similarly prepared from the reaction between 1 and methylhydrazine; the yield is 47%. IR (CH_2Cl_2), cm^{-1}: *ν*(CO) 1958 (vs), 1860 (vs), 1660 (vs); *ν*(C=N) 1605 (s). Mass (12 eV, ^{98}Mo), *m/z*: 318 (M^+). ^1H NMR (400 MHz, $CDCl_3$), *δ*: 1.88 (s, 3 H, CH_3), 2.86 (s, 3 H, CH_3), 5.39 (s, 5 H, C_5H_5), 6.92 (q, 1 H, C*H*Me) $J_{CH_3\text{-}H}$ = 5.6 Hz. ^{13}C NMR (100 MHz, $CDCl_3$), *δ*: 18.9 (CH_3), 25.8 (CH_3), 93.0 (C_5H_5), 145.0 (C=N), 199.3 (*C*O—N), 245.5, 255 (2 Mo—CO). Anal. Calcd for $C_{11}H_{12}MoO_3N_2$: C, 41.78; H, 3.82; H, 8.86. Found: C, 41.82; H, 3.86; N, 8.89.

Synthesis of $CpMo(CO)_2(\text{=C(OCH}_3\text{)NMe=CHCH}_3{\cdot}BPh_4$ (12). Complex 11 (0.50 g, 1.70 mmol) was dissolved in 20 mL of ether to which was added $CH_3CF_3SO_3$ (0.28 g, 1.70 mmol) to give an orange yellow solid. After filtration, the precipitate was washed with 20 mL of ether and dried in vacuo. The orange solid (0.70 g, 1.70 mmol) was dissolved in CH_3CN, $NaBPh_4$ (0.58 g, 1.70 mmol) was added, and the mixture was stirred for 12 h. After removal of CH_3CN, the residues were extracted twice with 20 mL of CH_2Cl_2. The extract was evaporated and recrystallized from saturated CH_2Cl_2/hexane to give dark red block crystals (61% yield, 0.68 g, 1.05 mmol). IR (CH_2Cl_2), cm^{-1}: 1992 (s), 1915 (s). ^1H NMR (400 MHz, CD_2Cl_2), *δ*: 1.53 (d, 3 H, CH_3), 2.44 (s, 3 H, N—CH_3), 4.15 (s, 3 H, OCH_3), 5.50 (s, 5 H, C_5H_5), 6.08 (q, 1 H, $CHCH_3$), 6.98–7.38 (complex m, 20 H, C_6H_5). ^{13}C NMR (100 MHz, CD_2Cl_2), *δ*: 18.9 (CH_3), 30.5 (N—CH_3), 65.5 (O—CH_3), 94.8 (C_5H_5), 122.3, 126.5, 136.5 (C_6H_5), 160.8 (C=N), 230.0, 245 (2 Mo—CO), 324.0 (M=$CCOCH_3$). Anal. Calcd for $C_{36}H_{35}MoO_3BN_2$: C, 66.52; H, 5.43; N, 4.30. Found: C, 66.50; H, 5.49; N, 4.40.

X-ray Diffraction Study of 6, 7, 10, and 12. Data were collected at room temperature on a CAD4 diffractometer, using graphite-monochromated Mo K*α* radiation. The structures were solved by the heavy-atom method; all data reduction and structural refinements were performed with the NRCCSDP package. Crystal data, details of data collection and structure analysis are summarized in Table V. For all structures, all non-hydrogen atoms were refined with anisotropic parameters. All hydrogen atoms included in the structure factor calculation were placed in idealized positions.

Acknowledgment. We thank the National Science Council for financial support of this work.

Supplementary Material Available: Listings of crystal data, bond lengths and angles, thermal parameters, and atom positional parameters for 6, 7, 10, and 12 (19 pages); listings of observed and calculated structure factors (47 pages). Ordering information is given on any current masthead page.